Kundu *et al. Carbon Research* (2024) 3:22
https://doi.org/10.1007/s44246-024-00108-1

Carbon Research

ORIGINAL ARTICLE

Open Access

Study of methylene blue dye removal using biochar derived from leaf and stem of *Lantana camara* L.

Deepa Kundu[1], Prabhakar Sharma[2,3*], Sayan Bhattacharya[1], Kaushik Gupta[4], Shubhalakshmi Sengupta[5] and Jianying Shang[6]

Abstract

The discharge of dye containing effluents into the water bodies has raised concern due to potential hazards related to their toxicity in the environment. The removal of dye from the aqueous solution can be efficiently performed using different kinds of adsorbents. The main objective of the current study is to determine the potential of biochar (BC) prepared from *Lantana camara* L. at 600 ℃ for the removal of methylene blue (MB) dye from aqueous solution as a function of contact time, pH (3–12), adsorbent dose (100–400 mg L^{-1}), and the initial dye concentration (5–20 mg L^{-1}). The BC prepared using leaf (BC_L600) and stem (BC_S600) of *Lantana* was characterized for elemental analysis, infrared spectroscopy, X-ray diffraction, scanning electron microscopy, and zeta potential analysis. The results indicated that the pH of dye solution had highly influenced their absorption over the BC surfaces. The pseudo-second-order kinetics was able to explain the interaction of MB dye with both BC_L600 and BC_S600, implying the multi-step characteristics of the adsorption process. It was also postulated through the thermodynamic analysis that the adsorption process was spontaneous and exothermic in nature. It implies that the adsorption mechanism was related to electrostatic, hydrogen bond, n-π, and π-π interactions, i.e., *Lantana* BC may be an effective bio-sorbent for the treatment of contaminated wastewater from the dye industries.

Highlights

- Equilibrium data obtained from batch experiment was fitted well with the Freundlich isotherm equation.
- Adsorption kinetics for MB dye was expressed by pseudo-second order model for BC pyrolyzed from *Lantana*.
- The possible mechanisms of dye adsorption were electrostatic, hydrogen-bond, n-π, and π-π interactions.
- *Lantana* biomass can be effectively used as an adsorbent to remove MB dye from aqueous solutions.

Keywords *Lantana* BC, Toxicity, Adsorption kinetics, Thermodynamics

Handling editor: Fengchang Wu.

*Correspondence:
Prabhakar Sharma
prabhakar.sharma@gmail.com
Full list of author information is available at the end of the article

Graphical Abstract

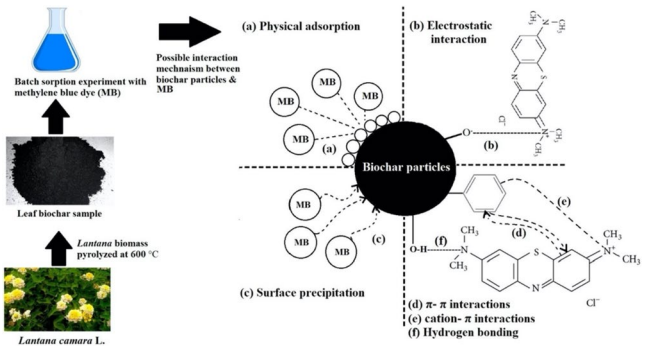

1 Introduction

The discharge of dyes containing wastewater from the leather, textile, paper, and plastics industries has emerged as a serious environmental concern due to their toxic and carcinogenic nature (Sharma et al. 2010). Methylene blue (MB) dye is a cationic dye generally used for dying cotton, wood, and silk (Deng et al. 2011). MB dye exposure can adversely affect human health, including skin and eye irritation, inhaled respiratory discomfort, and toxic reactions if ingested (Hameed & El-Khaiary 2008). It is crucial to handle it with care and avoid misuse. In medical settings, MB is used as a treatment for specific conditions under professional supervision, but improper exposure can lead to health issues. Additionally, its improper disposal can harm the environment, particularly aquatic life. Therefore, it is important to address the issue of wastewater pollution resulting from the discharge of dyes and identify an efficient removal technology for its suppression from industrial effluent.

Several separation technologies are employed to remove dyes from wastewater. The separation technologies for the removal of dyes from wastewater are classified under the categories of physical, chemical, and biological methods (Slokar & Majcen Le Marechal 1998). It can be separated by the commonly used method of coagulation and flocculation, where chemicals are added to form flocs that trap the dye particles. Among them, adsorption is preferred owing to its high removal efficiency and cost-effectiveness (Kulkarni et al. 2017). Adsorption involves materials like activated carbon or certain clays to adsorb dye molecules from the water. Also, it is an attractive method due to its design simplicity, ease of operation, insensitiveness towards toxic pollutants, and a smaller number of harmful substances (Rafatullah et al. 2010; Sharma et al. 2010). Membrane filtration, including techniques like ultrafiltration and reverse osmosis, can effectively remove dyes by physically blocking their passage. Biological treatments, such as activated sludge or constructed wetlands, use microorganisms to break down dyes. Each method has its advantages and limitations, and the choice depends on factors like the type of dye, its concentration, and the specific requirements of the wastewater treatment process.

Biochar has been recognized as a versatile and valuable material with a wide range of environmental applications. It is a byproduct obtained by the carbonization of biomass, which has emerged as an effective biosorbent for eradicating organic contaminants from the aqueous solution (Malik et al. 2017; Yang et al. 2019a, b; Yang et al. 2017a, b; Yang et al. 2017a, b). The physical and chemical properties of biochar are mainly governed by the feedstock type and pyrolysis temperature (Lehmann & Joseph 2009; Ok et al. 2015; Yang et al. 2019a, b). Feedstock can be obtained from agriculture, forestry, industrial waste, and sewage sludge (Shakya & Agarwal 2017). However, the physicochemical properties such as surface area, pH, and functional groups of biochar are highly dependent on the pyrolysis temperature (Ding et al. 2014; Yang et al. 2019a, b). The release of volatile matter may be intensified at the higher pyrolysis temperature, which ultimately may create more internal pores (Shaaban et al. 2014). Interestingly, the potential applications of biochar also include addressing global environmental issues such as climate change mitigation, carbon sequestration, contaminant immobilization, energy production, greenhouse gas reduction, soil amendment, and water purification (Abhishek et al. 2022; Ahmad et al. 2014; Lehmann & Joseph 2009). The unique properties of biochar such as large surface area having various functional groups, porous structure and mineral composition help to effectively remove the contaminants from the wastewater (Kumar et al. 2022; Nartey & Zhao 2014; Sinha et al. 2022a, b; Sinha et al. 2022a, b).

Lantana camara L., commonly known as *Lantana*, is an invasive weed (family Verbenaceae) primarily native to subtropical and tropical America except for a few taxa indigenous to tropical Asia and Africa (Negi et al. 2019). It has become a significant problem in many regions around the world after this plant was introduced to various countries as an ornamental garden plant due to its colorful flowers. In 1808, this plant species was also introduced to India as an ornamental plant at the National Botanical Garden (Hakimuddin 1930; Kohli et al. 2006). But later, it became a potential invader and adversely impacted the native plant species diversity and ecosystem functioning (Sharma et al. 2005; Sharma & Raghubanshi 2009). The aggressive growth and the ability to produce toxic compounds of *Lantana* deter herbivores and prolific seed production and allow them to escape cultivation and establish themselves in natural ecosystems. *Lantana* outcompetes native plants, disrupts ecological balance, and leads to habitat degradation. Controlling its spread is challenging, making it a serious concern for biodiversity conservation and land management efforts in affected areas. The invasion of *Lantana* in the forest ecosystems has adversely impacted the biodiversity via soil erosion (Day et al. 2003), nurturing vectors carrying communicable diseases (Syed & Guerin 2004), fostering fire fortuity (Hiremath & Sundaram 2005), and loss of native biodiversity due to allelopathic effect (Sharma et al. 2005). In order to manage the growth of the plant species, numerous control measures such as mechanical, chemical and biological have been employed (Negi et al. 2019), but none of them have been able to eradicate its invasion completely. Despite all, this notorious weed finds application in herbal medicine, industrial use, agricultural practices, phytoremediation and phytoextraction of heavy metals (Kumar et al. 2017; Sharma & Sharma 1989). Also, activated carbon synthesized from *Lantana* was effectively used as an adsorbent in order to remove tartrazine (Gautam et al. 2015), MB dye (Amuda et al. 2014), and phenol (Girish & Ramachandra Murty 2014) from aqueous solution.

The conversion of invasive species into biochar can significantly improve invasive plant management (Dong et al. 2013). It can also valorize its biomass for various environmental applications. Using biochar synthesized from the stem of *Lantana* invasive plant, MB dye removal was presented (Amuda et al. 2014), but a comparative analysis using their stem and leaf was not studied. Therefore, the main objective of this study was to examine the potential of biochar prepared from the leaf and stem of *Lantana* for the removal of MB dye from the aqueous solution as a function of solution chemistry, temperature, retention time, and absorbent doses. This was supplemented by kinetic isotherm, and thermodynamic modelling to better understand the correlation of MB dye interaction with biochar particles.

2 Materials and methods

2.1 Materials

MB dye with the molecular formula of $C_{16}H_{18}ClN_3S$ and molar mass of 319.85 g mol^{-1} was procured from "Sigma-Aldrich, India". A stock solution of 1.0 g L^{-1} of MB dye was prepared in deionized (DI) water and the working solutions were diluted with DI water using the stock solution. The concentration of the dye was determined at 610 nm wavelength using a UV–Vis spectrophotometer (Agilent Cary 100, USA). All chemicals utilized in the experiments were of analytical grade procured from "Sigma-Aldrich, India".

2.2 Preparation of leaf and stem biochar of Lantana

Lantana was collected from Tathagat Residential Hall (25°00′44.4"N 85°24′37.1"E), Nalanda University, Rajgir, Bihar, India. The plant materials were washed with tap water followed by DI water thrice. It was sun-dried for 10 h and crushed down to smaller pieces followed by washing with DI water thrice. The final powdered form of *Lantana* biomass was oven-dried (125 L-PID, Icon Instrument Company, India) at 120 ℃ for 24 h. The oven-dried biomass was pyrolyzed at 600 ℃ using a muffle furnace (Icon Instrument Company, India). The chosen temperature is within the temperature range reported for the preparation of *lantana camara* biochar (Chen et al. 2022; Ganesan et al. 2021). The BC samples prepared after the pyrolysis of *Lantana* were named BC_L600 and BC_S600 for leaves and stems, respectively. The samples were ground further using a ball mill to make the particle size uniform and stored in an air-tight glass bottle for batch experiments. Stock suspension of BC_L600 and BC_S600 were prepared by suspending the required amount of BC in double DI water. The BC suspensions were sonicated for 5 min using an Ultrasonic Cleaner (Olympus 10×50 DPS1, India) to completely homogenize the solution; however, the working concentrations were prepared daily with the requisite dilution.

2.3 Characterization of BC_L600 and BC_S600

The Infrared spectra of the unloaded BC_L600 and BC_S600 was obtained by using Fourier Transform Infrared Spectroscopy (Perkin Elmer-RZX, USA) to identify the surface functional groups in the wavenumber range of 400–4000 cm^{-1}. The Zeta potential and particle size (Zeta sizer Nano, ZS90, Malvern Instruments, USA) were determined in order to measure the magnitude of charges on the surface and external dimension of leaf and stem BC. The elemental composition (C, H, O, and

N) of the samples was assessed by an elemental analyzer (Vario EL III CHNOS Elemental Analyzer, USA). X-ray diffraction (XRD) analysis was performed to determine the sample's composition (Bruker, Germany). Scanning Electron Microscopy (SEM) was performed to understand the spatial variations in the chemical composition of BC and Energy Dispersive X-ray analysis (EDAX) was performed to find the presence of metals in addition to C and O in BC (FESEM-EDAX, JEOL, Japan).

2.4 Batch sorption experiments

The adsorptive removal efficiency of BC_L600 and BC_S600 prepared from *Lantana* for MB dye removal was examined by batch sorption experiments. Standard dye solutions of desired concentrations were prepared by diluting the stock solution. The pH of the MB dye solution was adjusted using 0.1 M HCl or 0.1 M NaOH solutions. Batch sorption experiments were performed by taking 50 mL of different dye concentrations (5, 10, 15 and 20 mg L^{-1}) in 250 mL of Erlenmeyer conical flasks at desired pH, contact time, and adsorbate concentrations. An absorbent dose of 250 mg L^{-1} and agitation rate of 150 rpm on a digital orbital shaker (WW5190020-Cole Parmer, USA) were used in the batch experiments. The sorption experiments were conducted at 303, 313 and 323 K temperature. The conical flasks were kept on the magnetic stirrer with a hot plate (Spinot-MC-02, India) along with the stirring bars. The temperature of the dye solution was maintained using a thermometer. The filtration and centrifugation techniques are common for separation of absorbent from the solution (Ganguly et al. 2020; Lyu et al. 2018). In this study, the adsorbent was segregated from the aqueous solution after equilibrium by centrifugation at 10,000 rpm for 10 min (Tarsons MC-01 Micro-centrifuge, India). All experiments were conducted in duplicate, and the averages of those results are presented in the manuscript.

3 Results and discussion

3.1 Characterization of BC_L600 and BC_S600

The particle size and elemental composition of BC_L600 and BC_S600 are presented in Table 1. The particle size of BC_L600 and BC_S600 was 517.2 ± 40.2 and 401.6 ± 4.2 nm, respectively. The elemental analysis of BC_L600 demonstrated that the percentage of oxygen is higher than that of carbon. Whereas the percentage of carbon in BC_S600 is exceptionally high as compared to the percentage of oxygen, which indicated the carbonaceous nature of the sorbent. The percentage of nitrogen is low in BC_S600 as compared to BC_L600. The zeta potential values of BC_L600 and BC_S600 were -31.7 ± 1.6 and -41.3 ± 1.4 mV at about neutral pH conditions. The zeta potential is an indicator of stability of colloidal dispersion. When the zeta potential value is low then the attractive forces overcome the repulsion leading to flocculation. A high value of zeta potential indicates electrically stabilized colloids resisting the flocculation. The stability of the colloids having zeta potential values exiting between 0 to ± 40 mV indicates low stability, while zeta potential values existing between ± 40 to ± 60 mV and above show good stability of the colloids (Greenwood & Kendall 1999). In the present study, the zeta potential value of BC_L600 is less than ± 40 mV indicating low stability of BC solution. Whereas BC_S600 solution is comparatively stable having zeta potential value slightly greater than ± 40 mV.

FTIR results played a vital role in elucidating the mechanisms of adsorption and provided valuable insights into the chemical structure of various compounds. The FTIR spectra of unloaded BC_L600 and BC_S600 is shown in Fig. 1 (A) and (B), respectively. In BC_L600 spectra, the band around 3300–3500 cm^{-1} and 1582 cm^{-1} were attributed due to surface with alcoholic or phenolic O − H stretching and bending mode of vibration. respectively. Due to the presence H-bond, the O–H stretching band is broad enough. Similar O–H stretching and bending modes of vibration were observed at around 3600–3200 cm^{-1} and 1570 cm^{-1}, respectively in the FTIR spectra of BC_S600 (Fig. 1B). From the broadness of IR spectra, the O–H bonds present in BC_S600 are more H-bond as compared to BC_L600. The bands observed between 1400–1600 cm^{-1} confirm the presence of C=C bond in both BC_L600 and BC_S600 spectra. The C − H bending vibrations were observed around 876.1, 820.9, 757.5 cm^{-1} in BC_L600 spectra and 874.5, 796.5, and 712.8 cm^{-1} in BC_S600 spectra. The C-H stretching vibrations are not observed in both FTIR spectra which is due to the predominant effect of O–H bands. The band around wavelength 1054.5 cm^{-1} in the BC_S600 spectra was associated with C − O stretching, which is very weak in case of BC_L600.

XRD pattern of samples BC_L600 and BC_S600 are shown in Fig. S1 within the °2θ range of 0–40°. The XRD

Table 1 Particle size and elemental composition of unloaded BC_L600 and BC_S600

BC type	Particle size (nm)	pH	N(%)	C(%)	H(%)	O(%)	H/C	O/C	Zeta potential (mV)
BC_L600	517.2 ± 40.2	7.1	2.99	41.84	1.95	53.23	0.046	1.27	-31.7 ± 1.6
BC_S600	401.6 ± 4.2	6.8	0.84	75.91	2.45	20.80	0.032	0.27	-41.3 ± 1.4

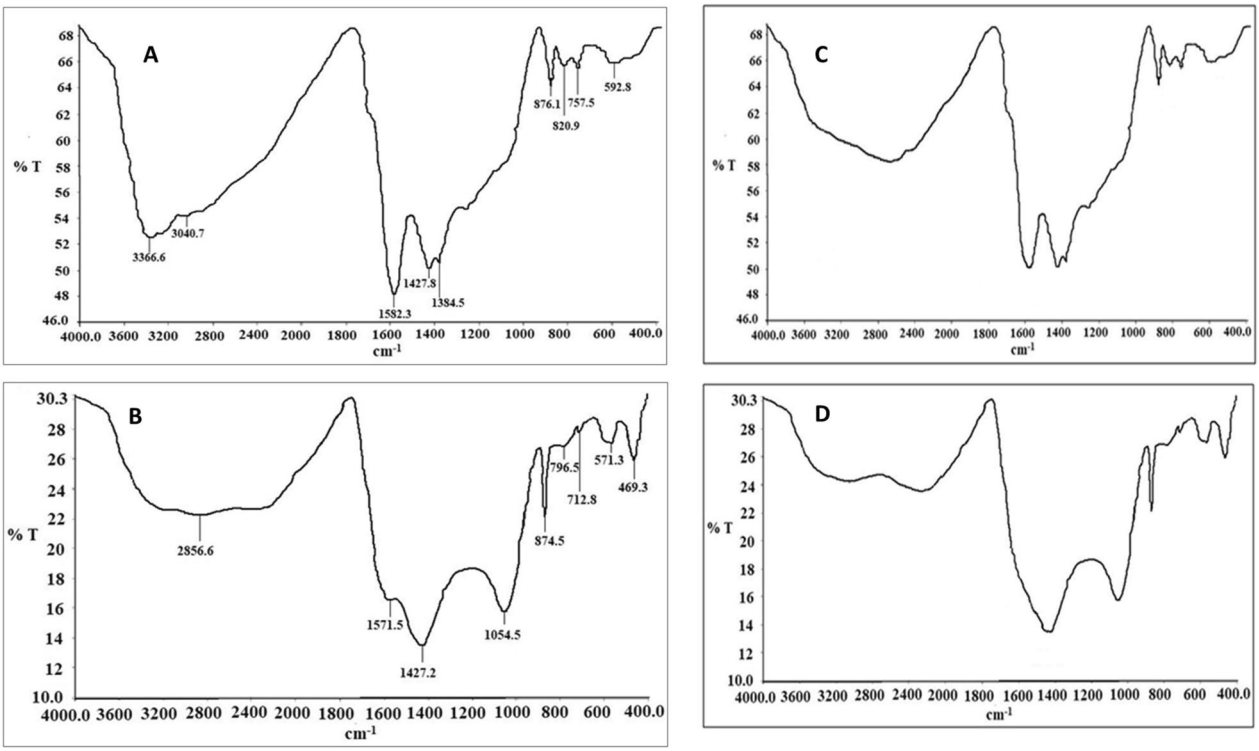

Fig. 1 FTIR spectra of (**A**) unloaded BC_L600, (**B**) unloaded BC_S600, (**C**) loaded BC_L600 and and (**B**) loaded BC_S600

patterns of both samples are different. In the XRD pattern of BC_L600, the numbers of peaks are larger than the XRD pattern of BC_S600 within the °2θ range of 0–40°. The peaks showed characteristic amorphous carbon XRD patterns. However, in BC_L600, additional peaks are observed due to the presence of crystalline phases of some oxides of different metals like Ca, Mg, Si (*i.e.,* CaO, MgO, SiO_2, respectively).

The SEM images elucidate the morphology and physical characteristics of the adsorbent. Figure 2 (A-F) shows the SEM images of BC_L600 and BC_S600 in two different magnifications. These images reveal the surface morphology of BC_L600 and BC_S600 samples. It is observed that the sizes of particles present in BC_L600 are higher than those in BC_S600 and the size distribution in BC_L600 is more homogeneous than BC_S600. The EDAX analysis explains the elemental composition of adsorbent and stipulate the types and amounts of elements present in the adsorbent, including the main constituents and impurities on the surface. It is useful for understanding the chemical nature of the adsorbent and its potential application in adsorption processes. The EDAX spectrums of both samples are shown in Fig. S2 (A, B). The EDAX spectrum of BC_L600 shows that the sample contains not only C and O but also Ca, Mg, and Si. The EDAX spectrum of BC_S600 shows that it contains only C and O.

3.2 Effect of initial dye concentration and contact time

Figure 3 illustrates the effect of "initial dye concentration" and "contact time" on the adsorption of MB dye onto BC_L600 and BC_S600. The amount of MB dye adsorbed on the surfaces of the adsorbent increased with increase in contact time due to the availability of number of active sites on the surfaces of adsorbents. As shown in Fig. 3, the dye solution treated with BC_L600 had attained equilibrium after ~ 100 min of contact time, whereas dye solution treated with BC_S600 attained equilibrium after ~ 60 min of contact time at constant pH 8. The adsorption equilibrium capacity had increased from 17.49 to 41.77 mg g^{-1} and 25.95 to 64.93 mg g^{-1} as the initial dye concentration was increased from 5 to 20 mg L^{-1} at 303 K with BC_L600 and BC_S600, respectively. After the diffusion of the dye molecules from the bulk solution to the surface of adsorbent particles, the adsorption process gradually slowed down until it attained equilibrium. This can be explained as a prominence of saturation of functional sites on the surface of adsorbents with the dye molecules and the penetration of dye molecules into the pores of the adsorbent structure. The interaction of dye molecules with the adsorbent was enhanced by increasing the dye concentrations as it overcomes the mass transfer resistance between the solid and aqueous phase (Gautam

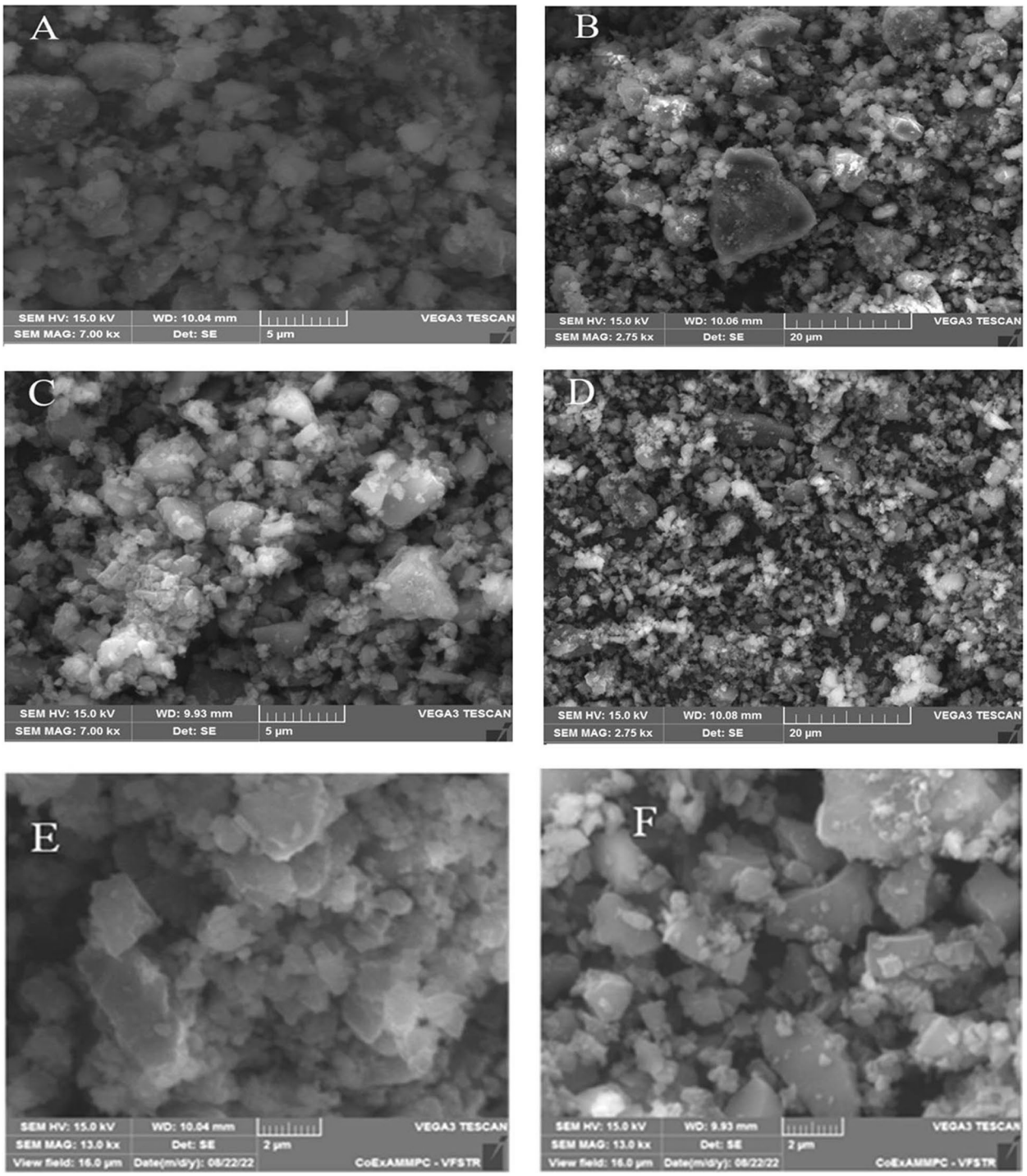

Fig. 2 SEM image of (**A**, **B**, **E**) BC_L600 and (**C**, **D**, **F**) BC_S600 with different resolutions

et al. 2015). Similar trend was reported on the sorption of MB on periodic mesoporous titanium phosphonate materials (Ren et al. 2013).

3.3 Effect of pH on the adsorption process

The effect of initial solution pH on the adsorption of MB dye by BC_L600 and BC_S600 was studied within the pH range of 3–12 and shown in Fig. 4. It was observed that the % removal of dye from aqueous solution increased

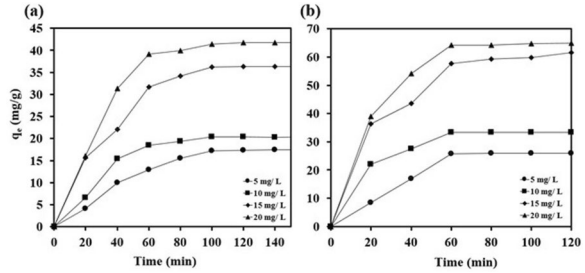

Fig. 3 Effect of initial dye concentration and contact time on adsorption of MB dye with (**A**) BC_L600 and (**B**) BC_S600 (Temperature = 303 K, pH = 8, Volume of MB dye = 40 ml, Contact time = 100 min, BC dose = 10 ml of 250 mg/L)

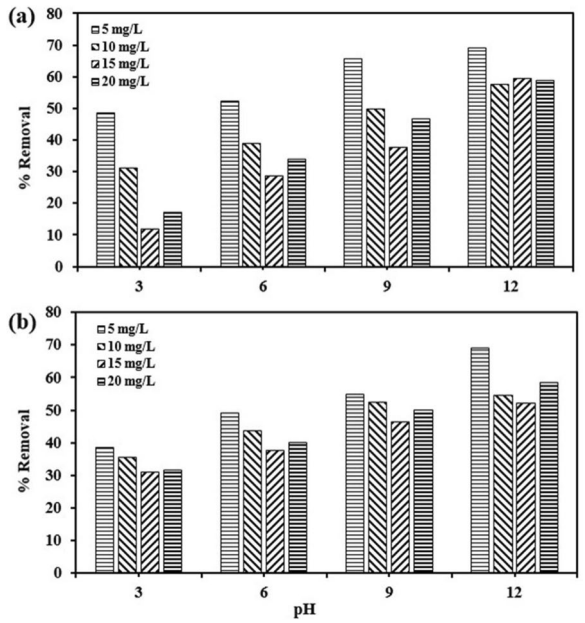

Fig. 4 Effect of initial solution pH of the sorption of MB dye onto (**A**) BC_L600 and (**B**) BC_S600(Temperature = 303 K, Volume of MB dye = 40 ml, Contact time = 100 min, BC dose = 10 ml of 250 mg/L) at different dye concentration

rapidly with the increasing pH from 3 to 12 by keeping all other experimental conditions constant. The results derived from the experimental data exhibit that the maximum uptake of MB dye occurred for 5 mg L^{-1} of BC at pH 12 with 69.02 and 69.07% using BC_L600 and BC_S600, respectively. The percentage removal of dye was 48.45, 52.13, and 65.72% and 38.38, 49.15, and 54.94% at pH 3, 6 and 9 for BC_L600 and BC_S600, respectively. The sorption mechanism is likely affected as a consequence of the electrostatic attraction and repulsion of dye molecules in the aqueous solution. At low pH, the sorption capacity of both the BC samples are low due the repulsive interaction between positively charged sorbent and positively charged sorbate. MB dye is a cationic dye (pKa = 3.80) and at low pH the BC surface remains predominantly cationic due to sorption of H^+ ions. With increase of solution pH, the sorbent surface become less and less positive. As a result, the sorption capacities of cationic MB dye increases. At high pH (~ 12), the surface of sorbent become negative, and a columbic attraction occurs between negatively charged sorbent and positively charged dye molecules (Hameed & Ahmad 2009). Raising the pH generally causes adsorbents to have more hydroxide ions and increases negative zeta potentials which facilitates the adsorption the cationic dye (i.e., MB dye) and removal from the media (Tarekegn et al. 2021). As a result, both the BC samples show very high dye sorption capacity at high pH. Similar results have been reported in adsorption of MB dye on steam-activated carbon prepared from *Lantana* stem (Amuda et al. 2014).

3.4 Effect of adsorbent dosage

Figure 5 shows the effect of adsorbent dose on the adsorption of MB dye over the BC_L600 and BC_S600 surfaces. The effect of adsorbent dose on the adsorption process was examined by ranging the adsorbent dose from 100 to 400 mg L^{-1} by keeping all other experimental condition constant at 303 K. The maximum amount of dye adsorbed on BC_L600 took place for initial dye concentration of 5 mg L^{-1} at pH 8 from 49.54 to 64.78% with an increase in adsorbent dose from 100 to 400 mg L^{-1}, respectively. Whereas the adsorption of MB dye on BC_S600 was maximum for initial dye concentration of 10 mg L^{-1} at pH 8 with 20.69 to 34.46% for adsorbent dose of 100 to 400 mg L^{-1}, respectively. The increase in removal efficiency can be attributed to the increase in available sorption sites (Ahmad et al. 2014). The adsorption of dye onto the surface of adsorbent is highly concentration dependent. The concentrations of MB dye used in the experiment are considerably low in the current study compared to the dosages of the adsorbent. It is possible that there could be more vacant sites available for adsorption until the reaction attains equilibrium. Therefore, the dye concentrations can be increased further until all the vacant sites are occupied by the dye molecules and become saturated. Similar trend was observed for MB dye adsorption with BC prepared from anaerobic digestion residue using palm bark, and eucalyptus (Sun et al. 2013), and steam-activated *Lantana camara* stem (Amuda et al. 2014). From Fig. 5, it is also observed that BC_L600 is an effective adsorbent at low dye concentration, whereas BC_S600 is effective at comparatively high dye concentration.

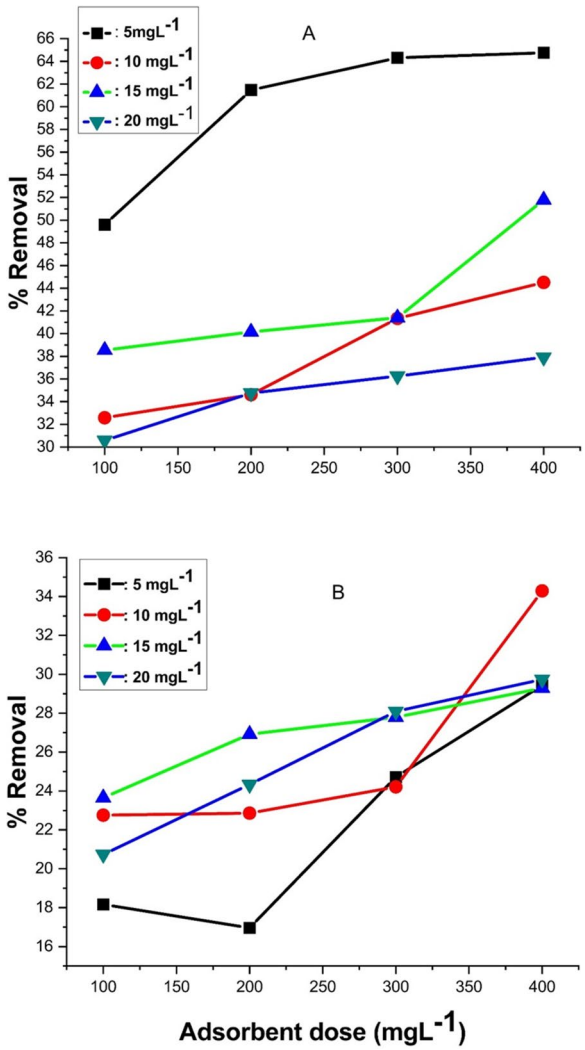

Fig. 5 Effect of adsorbent dose on the adsorption of MB dye with (**A**) BC_L600 and (**B**) BC_S600 (Temperature = 303 K, pH = 8 Volume of MB dye = 40 ml, Contact time = 100 min)

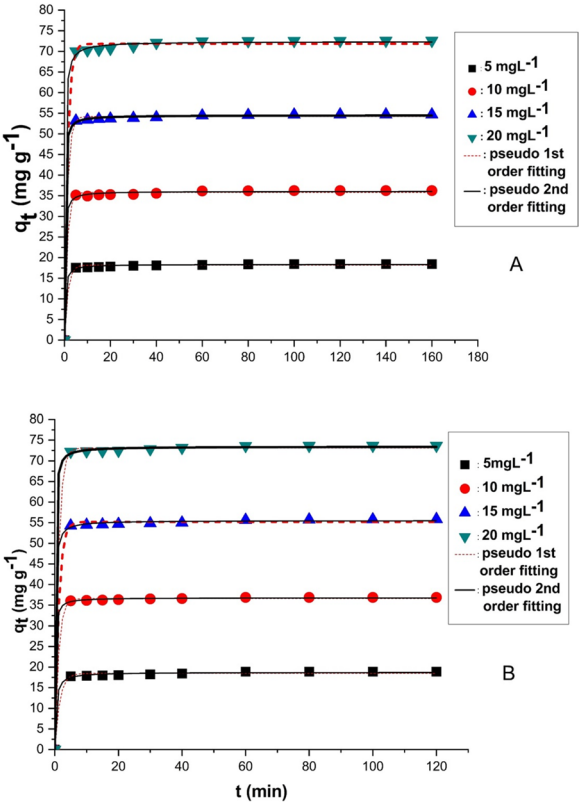

Fig. 6 Kinetic model fitting of adsorption of MB dye with (**A**) BC_L600 and (**B**) BC_S600(Temperature = 303 K, pH = 8 at different concentration

3.5 Adsorption kinetics

The sorption kinetic data were analyzed by nonlinear pseudo 1st order and pseudo 2nd order kinetic model equations (Eq. S3 and S5) and shown in Fig. 6. The kinetic parameters obtained are summarized in Table 2. From R^2 or χ^2values, it is clear that the sorption kinetics follows pseudo 2nd order kinetic model for both BC_L600 and BC_S600. From the rate constant values (k_2), it is shown that with increase of initial dye concentration rate of sorption reaction gradually decreases for both the adsorbent. This is due to the fact that with increase of initial dye concentration, the number of active sites on the sorbent per adsorbate molecules has decreased. Rate constant values are almost within the similar range for both the sorbents. Similar studies were reported for MB dye sorption kinetics on different adsorbents follows the pseudo 2nd order kinetic model (Kannan & Sundaram 2001; Rafatullah et al. 2010; Tran et al. 2020). Since present sorption reaction follows the pseudo 2nd order model for both the sorbents therefore the sorption process must be multistep process in which some diffusion steps must be involved.

3.6 Diffusion kinetics

The present kinetic data were analyzed by intraparticle diffusion model (Eq S6) and shown in Fig. S3. The results obtained are summarized in Table 3. From the Fig. S3 A and B, it is clear that for both BC_L600 and BC_S600 sorbents the q_t vs $t^{0.50}$ plot shows linearity from 5 min of contact time at all the concentrations studied. None of the linear plot passes through the origin. Thus, for the present sorption process, the intraparticle diffusion mechanism is operative but it is not involved in the rate limiting step (Suteu et al. 2015).

3.7 Adsorption isotherms

The adsorption equilibrium data at three different temperatures of MB dye for BC_L600 and BC_S600 were analyzed using non-linear Langmuir and Freundlich isotherm

Table 2 Parameters of two kinetic models for MB dye adsorption onto BC_L600 and BC_S600

BC zeta	MB initial concentration (mg L^{-1})	Pseudo-first-order				Pseudo-second-order			
		k_1 (min^{-1})	q_e^{cal} (mg g^{-1})	R^2	χ^2	k_2 (g mg^{-1} min^{-1})	q_e^{cal} (mg g^{-1})	R^2	χ^2
BC_L600	5	0.6634	18.18	0.9965	0.0886	0.1760	18.37	0.9988	0.0315
	10	0.7929	35.81	0.9974	0.2526	0.1357	36.08	0.9987	0.1301
	15	0.7865	54.22	0.9990	0.2227	0.1141	54.51	0.9996	0.0827
	20	0.7295	71.83	0.9979	0.8304	0.0608	72.39	0.9992	0.3199
BC_S600	5	0.6460	18.46	0.9950	0.1540	0.1498	18.72	0.9978	0.0685
	10	0.8354	36.61	0.9994	0.0740	0.1285	36.79	0.9998	0.0275
	15	0.8170	55.19	0.9989	0.2906	0.1191	55.50	0.9995	0.1405
	20	0.8769	73.09	0.9994	0.3163	0.1160	73.45	0.9997	0.1473

Table 3 Intraparticle diffusion model parameters of MB dye sorption on BC_L600 and BC_S600

Parameters	BC_L600				BC_S600			
Concentration (mgL^{-1})	5	10	15	20	5	10	15	20
k_{id}($mgg^{-1}min^{0.50}$)	0.0945	0.1416	0.1513	0.2728	0.1449	0.1535	0.1994	0.2017
C	17.4340	34.7197	53.0217	69.6808	17.4747	35.8951	53.8358	71.7262
χ^2	0.0980	0.3815	0.2543	1.7970	0.1329	0.0766	0.1512	0.2884
R^2	0.9199	0.8680	0.9189	0.8377	0.9182	0.9085	0.9494	0.9092

models equations (Eqs S6 and S8). The fitted curves are shown in Fig. 7. The isotherm parameters obtained by this analysis are summarized in Table 4. Comparison of R^2 or χ^2 values clearly indicates that sorption of MB dye on both BC_L600 and BC_S600 follows Langmuir sorption isotherm at all the temperature studied. It indicates a homogeneous distribution of active sites on the surface of BC resulting in the formation of monolayer coverage of MB dye at a given temperature. Maximum sorption capacity (q_m) of BC_L600 and BC_S600 are 64.99 and 15.39 mg g^{-1}, respectively at 303 K. Thus, it is clear from q_m values that BC_L600 shows a fairly high sorption capacity than BC_S600. From Table 4 it is seen that maximum sorption capacity gradually decreases with increase of temperature for both the sorbents. This indicates the exothermic nature of the sorption process. The separation factor (R_L) values are calculated (Eq S7) for MB dye adsorption on both the sorbents at all the temperatures studied and presented in Table 4. The R_L values for all the sorption processes lie within the range > 0 and < 1 which indicates favorable adsorption conditions (Bulut & Aydın, 2006).

A comparative study of maximum Langmuir sorption capacities of different adsorbents applied for MB dye sorption with the adsorbents had been performed and presented in Table 5. Comparing the sorption capacity of different adsorbents with the BC_L600 and BC_S600 further determines the potential of using BC_L600 to produce BC for the effective removal of MB. Adsorbents such as activated carbon developed from *Ficus carica* bast (Pathania et al. 2017), Polyaniline and Polypyrrole Macro– nanoparticles (Maruthapandi et al. 2018) and Dunino raw halloysite mineral (Filice et al. 2021) have reported low q_m values than BC_L600 for the effective removal of MB dye.

3.8 Thermodynamics of the adsorption process

The spontaneity of the adsorption process was determined by thermodynamic studies. Gibb's free energy change (ΔG^0) indicates the spontaneity of any process. At a given temperature, the adsorption processes occur spontaneously if ΔG^0 is negative. It is required to take into account both the enthalpy (ΔH^0) and the entropy (ΔS^0) while computing ΔG^0. An exothermic adsorption is shown by a negative value for ΔH^0, whereas an endothermic adsorption is indicated by a positive value. Different thermodynamic parameters are calculated using Eqs S9 and S10. The plot of *ln*K vs 1/T is shown in Fig. S4. Thermodynamic parameters of MB dye sorption on BC_L600 and BC_S600 are presented in Table 6. In the present study, the negative values of ΔG^0atallthethree temperatures studied shows that, the dye adsorption onto BC_L600 and BC_S600 are favorable under the experimental conditions (Sumalinog et al. 2018). Decrease of ΔG^0 values with increase in temperature for both sorbents indicates

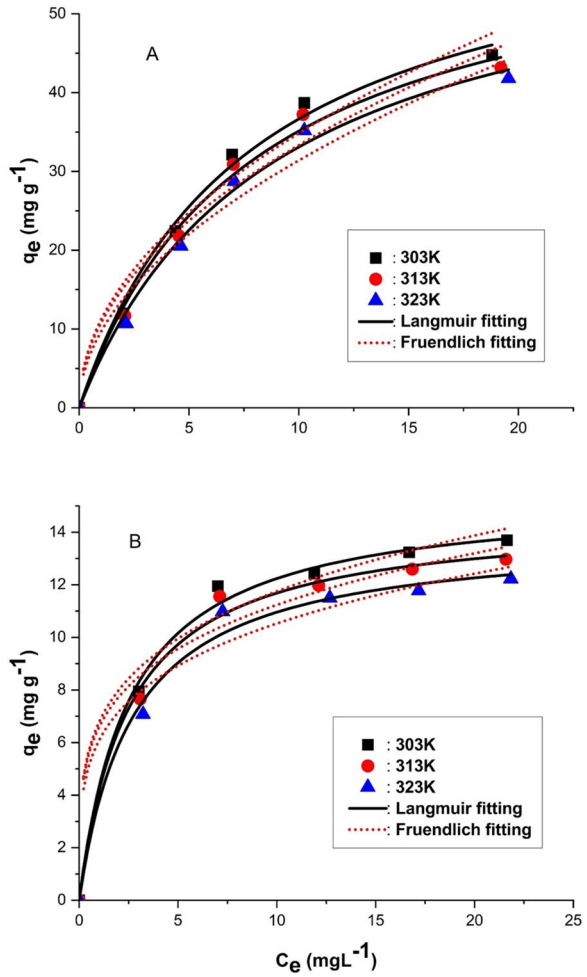

Fig. 7 Isotherm study of MB dye on (**A**) BC_L600 and (**B**) BC_S600(pH = 8) and Freundlich, Langmuir sorption isotherm fitting

that the sorption is more favorable at higher temperature conditions. The negative values of ΔH^0 confirmed the exothermic nature of the sorption process. The estimated values for change in enthalpy are lower than 40 kJ mol^{-1}for both sorbents. This clearly indicates that the forces involved between the adsorbate and absorbent is van der Waals' type resulting in physical adsorption (Fan et al. 2016). Thus, it can be inferred that the interaction mechanism between the MB dye and BC is mainly physical adsorption in the current study. The positive ΔS^0 values suggest an increase in the degree of randomness at the solid/solution interface, which is comparatively higher in case of dye adsorption onto BC_S600 than BC_L600 during the sorption process. This observation is in accordance with MB dye adsorption onto activated BC produced from municipal solid waste (Sumalinog et al. 2018).

3.9 Mechanisms of interaction

The possible mechanism of dye adsorption on BC prepared from *Lantana camara* L. can be determined by combining the results of adsorption and infrared spectroscopy analyses. The interaction of hydroxyl-group presents on the surface of BC_L600 and BC_S600 with MB dye molecules in the solution is related to intermolecular hydrogen bonding. In alkaline conditions, the hydroxyl-group increases in the solution by enhancing the interaction of dye molecules with the BC. The presence of aromatic carbon on both BC_L600 and BC_S600 indicated the hydrophobic nature of the adsorbents. The presence of C = C and C − H groups indicated the presence of benzene like structure on the surface of BC_L600 and BC_S600. The structure of MB dye contains three aromatic rings which allow the π-π interaction with both BC_L600 and BCs600 since their surfaces also contains benzene like structures. The cation of the thiazine group is present in the middle of two aromatic rings comprising of dimethyl amide in the MB dye structure, which possibly have interacted with the π system of the BC. The presence of C − O on the surface of BC_S600 can interact by developing an electrostatic bond with the cationic dye molecules. The N atoms of two 2° amine groups present in the structure of MB dye can form H-bonds with the surface O–H groups of BC samples. As a result of the fact

Table 4 Parameters of adsorption isotherms of MB dye onto BC_L600 and BC_S600

BC	Tempt. (K)	Langmuir Isotherm					Freundlich Isotherm			
		q_m (mg g^{-1})	K_L (L mg^{-1})	R_L	χ^2	R^2	K_F (mg g^{-1})	n	χ^2	R^2
	303	64.99	0.1294	0.2361	2.2879	0.9920	11.22	2.03	14.4465	0.9151
BC_L600	313	62.67	0.1275	0.2388	2.4907	0.9906	10.81	2.04	14.2984	0.9083
	323	62.25	0.1135	0.2605	2.0525	0.9916	9.71	1.96	12.2116	0.9180
	303	15.39	0.3983	0.0934	0.1655	0.9940	6.77	4.18	0.7718	0.8523
BC_S600	313	14.62	0.3887	0.0912	0.1944	0.9923	6.59	4.31	0.8194	0.8205
	323	13.92	0.3699	0.0976	0.2596	0.9885	6.08	4.19	0.9357	0.7841

Table 5 Comparison of maximum Langmuir sorption capacity (q_m) of different adsorbents

Adsorbent	q_m (mgg^{-1})	Reference
BC_L600	64.99	**Present study**
BC_S600	15.39	**Present study**
Corn-husk	47.95	(Paşka et al. 2014)
Activated carbon developed from *Ficus carica* bast	47.62	(Pathania et al. 2017)
Sawdust	76.92	(Markandeya et al. 2015)
Polyaniline and Polypyrrole Macro–nanoparticles	19.67, 19.96	(Maruthapandi et al. 2018)
Dunino raw halloysite mineral	10.55	(Filice et al. 2021)
Carbon nanotubes	46.20	(Yao et al. 2010)
Polyaniline nanotubesbase	9.21	(Chen et al. 2014)
Natural zeolite	19.94	(Han et al. 2009)

Table 6 Thermodynamic parameters of sorption of MB dye onto BC_L600 and BC_S600

BC	Temperature (℃)	ΔG^0 (kJ mol^{-1})	ΔH^0 ((kJ mol^{-1})	ΔS^0 ((kJ mol^{-1} K^{-1})
BC_L600	30	-12.25	-5.37	+0.0229
	40	-12.62		
	50	-12.71		
BC_S600	30	-15.08	-3.02	+0.0398
	40	-15.52		
	50	-15.88		

the intensities of O–H stretching mode of vibrations are lowered to a large extent (Fig. 1 C, D). Similar interactions have been reported previously for MB dye interaction with activated carbon, graphene oxide, and carbon nanotubes (Li et al. 2013). It is likely that the dye molecules can physically interact with the surface moieties of both the adsorbents prepared from *Lantana* in the current study. A schematic representation of different interactions of MB dye with BC samples are presented in Fig. 8. It highlights the hydrogen bonding, electrostatic

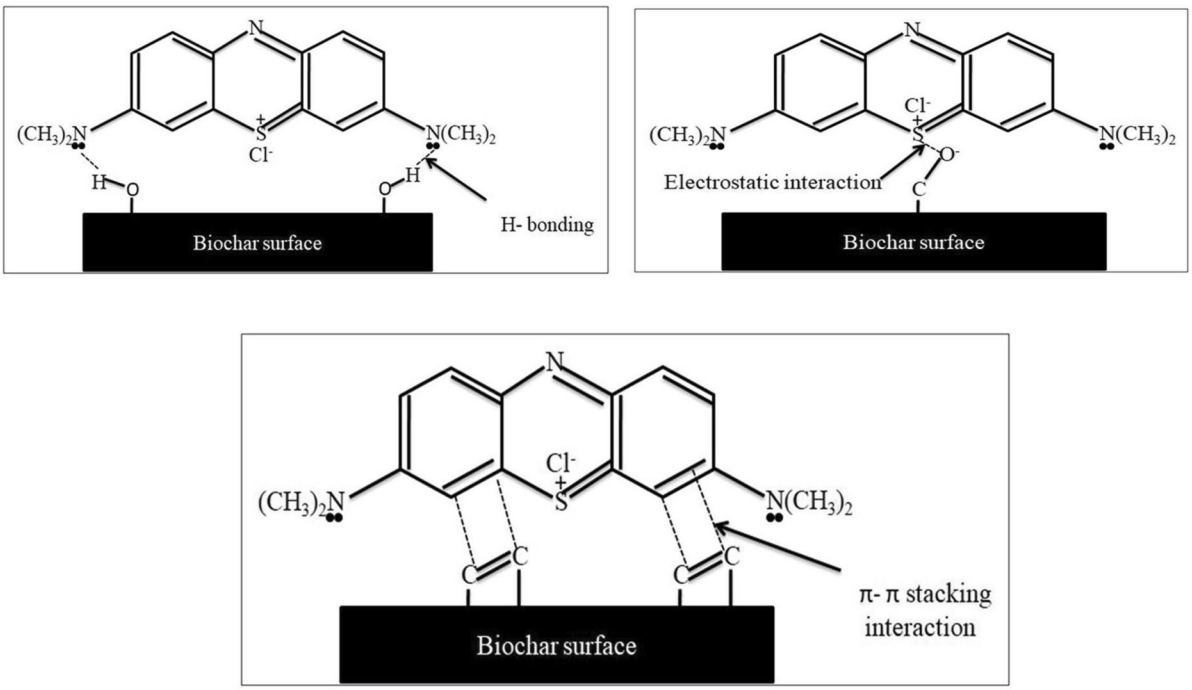

Fig. 8 Different types of interactions between methylene blue and biochar surface

interaction, and stacking interaction, respectively over the BC surfaces.

4 Conclusions

Through the adsorption potential of BC prepared from *Lantana* biomass, the adsorption of dye onto BC_L600 and BC_S600 was found to be highly dependent on the pH of the solution. It was observed that the adsorption of dye molecules onto BC_L600 and BC_S600 had significantly increased with the increase in pH from 3 to 12. The amount of dye adsorbed by BC_L600 was found to be high as compared to that of BC_S600 possibly due to the presence of surface –O–H and C–O functional groups. It was also noted that the dye analyzed with BC_L600 acquired equilibrium in ~ 100 min only whereas, the dye treated with BC_S600 attained equilibrium in about 60 min. The rate of sorption for both BC_L600 and BC_S600 was following the "pseudo-second-order" kinetics. It implies that the adsorption of dye molecules onto the surface of BC is a multi-step process involving external adsorption as well as diffusion of the dye molecules into the interior of the adsorbent. The equilibrium data fitted very well in the Langmuir isotherm equation for both the adsorbents, confirming multilayer adsorption capacity with BC_L600 and BC_S600. The negative values of both ΔG^0 and ΔH^0 for the sorption processes suggest that the adsorption processes are spontaneous and exothermic in nature. The positive values of ΔS^0 signified a higher degree of randomness in the system comprising BC and dye molecules.

Thus, this study goes a step further from previous works carried out by Amuda et al. (2014), as both the biomass of this invasive species has been studied and dye adsorption properties of the biochar derived from stem was also ascertained. BCL600 prepared from leaves had higher dye absorption capacity although it reached equilibrium at ~ 100 min where as BCS600 reached it at about 60 min. This implies effective utilization of the entire biomass of an invasive species. The surface of BC can be further modified depending on the types of contaminants present in their surroundings. Therefore, it can be anticipated that the BC particles obtained from Lantana camara L. biomass can be applied as a potential adsorbent for water and wastewater treatment.

Abbreviation

MB	Methylene blue
BC	Biochar
BC_L600	Leaf biochar pyrolyzed at 600 ℃
BC_S600	Stem biochar pyrolyzed at 600 ℃
C_0	Initial adsorbate concentration (mg L^{-1})
C_e	Equilibrium adsorbate concentration (mg L^{-1})
q_t	Adsorbate concentration (mg g^{-1}) at time, t (min)
q_e	Equilibrium adsorbate concentration (mg g^{-1})
q_0	Maximum adsorption capacity (mg g^{-1})
R^2	Linear regression correlation coefficient
K_L	Langmuir isotherm coefficient (L mg^{-1})
R_L	Dimensionless separation factor
K_F	Freundlich isotherm coefficient (mg g^{-1})
M	Mass of the adsorbent (g)
V	Volume of the solution (L)
Exp	Experimental
Cal	Calculated

Supplementary Information

The online version contains supplementary material available at https://doi.org/10.1007/s44246-024-00108-1.

Supplementary material 1.

Acknowledgements

We greatly acknowledge the support from FTIR laboratory, Punjab University, Chandigarh, India for offering the laboratory facilities to carry out the FTIR analysis.

Authors' contributions

Deepa Kundu: Conceptualization, experiments, writing first draft. Prabhakar Sharma: Conceptualization, supervision, writing, editing, reviewing. Sayan Bhattacharya: Writing, review and editing. Kaushik Gupta: Writing –review and editing, developing diagrams. Shubhalakshmi Sengupta: SEM image analysis, review and editing. Jianying Shang: Review and editing.

Funding

This study has not received any funding.

Availability of data and materials

All data, models, and code generated or used during the study appear in the submitted article.

Declarations

Competing interests

The authors declare that they have no known competing financial interests or personal relationships that could have appeared to influence the work reported in this paper.

Author details

[1]School of Ecology and Environment Studies, Nalanda University, Rajgir, Nalanda, Bihar, India. [2]Department of Agricultural Engineering and Technology, School of Engineering and Technology, Nagaland University, Dimapur, Nagaland, India. [3]Lok Prerna, Deoghar, Jharkhand, India. [4]Belur High School (H.S), Howrah, West Bengal, India. [5]Department of Chemistry, School of Applied Science and Humanities, Vignan's Foundation for Science Technology and Research (VFSTR) Deemed to Be University, Vadlamudi, Guntur, Andhra Pradesh 522213, India. [6]Department of Soil and Water Sciences, China Agricultural University, Beijing, PR China.

Received: 14 September 2023 Revised: 30 January 2024 Accepted: 3 February 2024
Published online: 07 March 2024

References

Abhishek K, Shrivastava A, Vimal V, Gupta AK, Bhujbal SK, Biswas JK, Singh L, Ghosh P, Pandey A, Sharma P, Kumar M (2022) Biochar application for greenhouse gas mitigation, contaminants immobilization and soil fertility enhancement: a state-of-the-art review. Sci Total Environ 853:158562. https://doi.org/10.1016/j.scitotenv.2022.158562

Ahmad M, Rajapaksha AU, Lim JE, Zhang M, Bolan N, Mohan D, Vithanage M, Lee SS, Ok YS (2014) Biochar as a sorbent for contaminant management in soil and water: a review. Chemosphere 99:19–33. https://doi.org/10.1016/j.chemosphere.2013.10.071

Amuda OS, Olayiwola AO, Alade AO, Farombi AG, Adebisi SA (2014) Adsorption of methylene blue from aqueous solution using steam-activated carbon produced from Lantana camara stem. J Environ Prot 05(13):1352–1363. https://doi.org/10.4236/jep.2014.513129

Bulut Y, Aydın H (2006) A kinetics and thermodynamics study of methylene blue adsorption on wheat shells. Desalination 194(1–3):259–267. https://doi.org/10.1016/j.desal.2005.10.032

Chen Z, Fu J, Wang M, Wang X, Zhang J, Xu Q (2014) Adsorption of cationic dye (methylene blue) from aqueous solution using poly(cyclotriphosphazene-co-4,4′-sulfonyldiphenol) nanospheres. Appl Surf Sci 289:495–501. https://doi.org/10.1016/j.apsusc.2013.11.022

Chen K, Ma D, Yu H, Zhang S, Seyler BC, Chai Z, Peng S (2022) Biosorption of V(V) onto Lantana camara biochar modified by H3PO4: Characteristics, mechanism, and regenerative capacity. Chemosphere 291:132721. https://doi.org/10.1016/j.chemosphere.2021.132721

Day MD, Wiley CJ, Playford J, Zalucki MP (2003) Lantana: current management status and future prospects

Deng H, Lu J, Li G, Zhang G, Wang X (2011) Adsorption of methylene blue on adsorbent materials produced from cotton stalk. Chem Eng J 172(1):326–334. https://doi.org/10.1016/j.cej.2011.06.013

Ding W, Dong X, Ime IM, Gao B, Ma LQ (2014) Pyrolytic temperatures impact lead sorption mechanisms by bagasse biochars. Chemosphere 105:68–74. https://doi.org/10.1016/j.chemosphere.2013.12.042

Dong X, Ma LQ, Zhu Y, Li Y, Gu B (2013) Mechanistic investigation of mercury sorption by Brazilian pepper biochars of different pyrolytic temperatures based on x-ray photoelectron spectroscopy and flow calorimetry. Environ Sci Technol 47(21):12156–12164. https://doi.org/10.1021/es4017816

Fan S, Tang J, Wang Y, Li H, Zhang H, Tang J, Wang Z, Li X (2016) Biochar prepared from co-pyrolysis of municipal sewage sludge and tea waste for the adsorption of methylene blue from aqueous solutions: Kinetics, isotherm, thermodynamic and mechanism. J Mol Liq 220:432–441. https://doi.org/10.1016/j.molliq.2016.04.107

Filice S, Bongiorno C, Libertino S, Compagnini G, Gradon L, Iannazzo D, La Magna A, Scalese S (2021) Structural characterization and adsorption properties of dunino raw halloysite mineral for dye removal from water. Materials 14(13):3676. https://doi.org/10.3390/ma14133676

Ganesan S, Eswaran M, Chokkiah B, Dhanusuraman R, Lingassamy AP, Ponnusamy VK, Kumar G, Pugazhendhi A (2021) Facile and low-cost production of Lantana camara stalk-derived porous carbon nanostructures with excellent supercapacitance and adsorption performance. Int J Energy Res 45(12):17440–17449. https://doi.org/10.1002/er.5730

Ganguly P, Sarkhel R, Das P (2020) Synthesis of pyrolyzed biochar and its application for dye removal: batch, kinetic and isotherm with linear and non-linear mathematical analysis. Surf Interfaces 20:100616. https://doi.org/10.1016/j.surfin.2020.100616

Gautam RK, Gautam PK, Banerjee S, Rawat V, Soni S, Sharma SK, Chattopadhyaya MC (2015) Removal of tartrazine by activated carbon biosorbents of Lantana camara: kinetics, equilibrium modeling and spectroscopic analysis. J Environ Chem Eng 3(1):79–88. https://doi.org/10.1016/j.jece.2014.11.026

Girish CR, Ramachandra Murty V (2014) Adsorption of phenol from aqueous solution using *Lantana camara*, forest waste: Kinetics, isotherm, and thermodynamic studies. Int Sch Res Notices 2014:1–16. https://doi.org/10.1155/2014/201626

Greenwood R, Kendall K (1999) Selection of suitable dispersants for aqueous suspensions of zirconia and titania powders using acoustophoresis. J Eur Ceram Soc 19(4):479–488. https://doi.org/10.1016/S0955-2219(98)00208-8

Hakimuddin M (1930) Lantana in Northern India as a pest and its probable utility in solving the cowdung problem. Indian Forester 56(9):405–410

Hameed BH, Ahmad AA (2009) Batch adsorption of methylene blue from aqueous solution by garlic peel, an agricultural waste biomass. J Hazard Mater 164(2–3):870–875. https://doi.org/10.1016/j.jhazmat.2008.08.084

Hameed BH, El-Khaiary MI (2008) Removal of basic dye from aqueous medium using a novel agricultural waste material: Pumpkin seed hull. J Hazard Mater 155(3):601–609. https://doi.org/10.1016/j.jhazmat.2007.11.102

Han R, Zhang J, Han P, Wang Y, Zhao Z, Tang M (2009) Study of equilibrium, kinetic and thermodynamic parameters about methylene blue adsorption onto natural zeolite. Chem Eng J 145(3):496–504. https://doi.org/10.1016/j.cej.2008.05.003

Hiremath AJ, Sundaram B (2005) The Fire-Lantana cycle hypothesis in Indian forests. Conserv Soc 3:26–42

Kannan N, Sundaram MM (2001) Kinetics and mechanism of removal of methylene blue by adsorption on various carbons—a comparative study. Dyes Pigm 51(1):25–40. https://doi.org/10.1016/S0143-7208(01)00056-0

Kohli RK, Batish DR, Singh HP, Dogra KS (2006) Status, invasiveness and environmental threats of three tropical American invasive weeds (Parthenium hysterophorus L., Ageratum conyzoides L., Lantana camara L.) in India. Biological Invasions 8(7):1501–1510. https://doi.org/10.1007/s10530-005-5842-1

Kulkarni MR, Revanth T, Acharya A, Bhat P (2017) Removal of Crystal Violet dye from aqueous solution using water hyacinth: Equilibrium, kinetics and thermodynamics study. Resource-Efficient Technologies 3(1):71–77. https://doi.org/10.1016/j.reffit.2017.01.009

Kumar G, Shobana S, Chen WH, Bach QV, Kim SH, Atabani AE, Chang JS (2017) A review of thermochemical conversion of microalgal biomass for biofuels: chemistry and processes. Green Chem 19(1):44–67. https://doi.org/10.1039/C6GC01937D

Kumar R, Sharma P, Yang W, Sillanpää M, Shang J, Bhattacharya P, Vithanage M, Maity JP (2022) State-of-the-art of research progress on adsorptive removal of fluoride-contaminated water using biochar-based materials: Practical feasibility through reusability and column transport studies. Environ Res 214. https://doi.org/10.1016/j.envres.2022.114043

Lehmann J, Joseph S (2009) Biochar for environmental management: an introduction. In: Lehmann J, Joseph S (eds) Biochar for environmental management: science, technology, and implementation. Earthscan, pp 1–12

Li Y, Du Q, Liu T, Peng X, Wang J, Sun J, Wang Y, Wu S, Wang Z, Xia Y, Xia L (2013) Comparative study of methylene blue dye adsorption onto activated carbon, graphene oxide, and carbon nanotubes. Chem Eng Res Des 91(2):361–368. https://doi.org/10.1016/j.cherd.2012.07.007

Lyu H, Gao B, He F, Zimmerman AR, Ding C, Tang J, Crittenden JC (2018) Experimental and modeling investigations of ball-milled biochar for the removal of aqueous methylene blue. Chem Eng J 335:110–119. https://doi.org/10.1016/j.cej.2017.10.130

Malik DS, Jain CK, Yadav AK, Banerjee S (2017) Role of plant-based biochar in pollutant removal: an overview. Advanced materials for wastewater treatment. Wiley, pp 313–330. https://doi.org/10.1002/9781119407805.ch9

Markandeya Singh A, Shukla SP, Mohan D, Singh NB, Bhargava DS, Shukla R, Pandey G, Yadav VP, Kisku GC (2015) Adsorptive capacity of sawdust for the adsorption of MB dye and designing of two-stage batch absorber. Cogent Environ Sci 1(1):1075856. https://doi.org/10.1080/23311843.2015.1075856

Maruthapandi M, Kumar VB, Luong JHT, Gedanken A (2018) Kinetics, isotherm, and thermodynamic studies of methylene blue adsorption on polyaniline and polypyrrole macro–nanoparticles synthesized by C-dot-initiated polymerization. ACS Omega 3(7):7196–7203. https://doi.org/10.1021/acsomega.8b00478

Nartey OD, Zhao B (2014) Biochar preparation, characterization, and adsorptive capacity and its effect on bioavailability of contaminants: an overview. Adv Mater Sci Eng 2014:1–12. https://doi.org/10.1155/2014/715398

Negi GCS, Sharma S, Vishvakarma SCR, Samant SS, Maikhuri RK, Prasad RC, Palni LMS (2019) Ecology and use of Lantana camara in India. Bot Rev 85(2):109–130. https://doi.org/10.1007/s12229-019-09209-8

Ok YS, Uchimiya SM, Chang SX, Bolan N (Eds.). (2015). Biochar: Production, characterization, and applications (1st ed.). CRC Press, Boca Raton. https://doi.org/10.1201/b18920.

Paşka OM, Păcurariu C, Muntean SG (2014) Kinetic and thermodynamic studies on methylene blue biosorption using corn-husk. RSC Adv 4(107):62621–62630. https://doi.org/10.1039/C4RA10504D

Pathania D, Sharma S, Singh P (2017) Removal of methylene blue by adsorption onto activated carbon developed from Ficus carica bast. Arab J Chem 10:S1445–S1451. https://doi.org/10.1016/j.arabjc.2013.04.021

Rafatullah M, Sulaiman O, Hashim R, Ahmad A (2010) Adsorption of methylene blue on low-cost adsorbents: a review. J Hazard Mater 177(1–3):70–80. https://doi.org/10.1016/j.jhazmat.2009.12.047

Ren T-Z, Zhu X-H, Ma T-Y, Yuan Z-Y (2013) Adsorption of methylene blue from aqueous solution by periodic mesoporous titanium phosphonate materials. Adsorpt Sci Technol 31(6):535–548. https://doi.org/10.1260/0263-6174.31.6.535

Shaaban A, Se S-M, Dimin MF, Juoi JM, Mohd Husin MH, Mitan NMM (2014) Influence of heating temperature and holding time on biochars derived from rubber wood sawdust via slow pyrolysis. J Anal Appl Pyrol 107:31–39. https://doi.org/10.1016/j.jaap.2014.01.021

Shakya A, Agarwal T (2017) Poultry litter biochar: an approach towards poultry litter management – A review. Int J Curr Microbiol Appl Sci 6(10):2657–2668. https://doi.org/10.20546/ijcmas.2017.610.314

Sharma GP, Raghubanshi AS (2009) Lantana invasion alters soil nitrogen pools and processes in the tropical dry deciduous forest of India. Appl Soil Ecol 42(2):134–140. https://doi.org/10.1016/j.apsoil.2009.03.002

Sharma OP, Sharma PD (1989) Natural products of the lantana plant - the present and prospects. J Sci Ind Res 48(10):471–478

Sharma GP, Raghubanshi AS, Singh JS (2005) *Lantana* invasion: an overview. Weed Biol Manag 5(4):157–165. https://doi.org/10.1111/j.1445-6664.2005.00178.x

Sharma YC, Uma, Sinha ASK, Upadhyay SN (2010) Characterization and adsorption studies of Cocos nucifera L. activated carbon for the removal of methylene blue from aqueous solutions. J Chem Eng Data 55(8):2662–2667. https://doi.org/10.1021/je900937f

Sinha R, Kumar R, Abhishek K, Shang J, Bhattacharya S, Sengupta S, Kumar N, Singh RK, Mallick J, Kar M, Sharma P (2022a) Single-step synthesis of activated magnetic biochar derived from rice husk for hexavalent chromium adsorption: Equilibrium mechanism, kinetics, and thermodynamics analysis. Groundw Sustain Dev 18. https://doi.org/10.1016/j.gsd.2022.100796

Sinha R, Kumar R, Sharma P, Kant N, Shang J, Aminabhavi TM (2022b) Removal of hexavalent chromium via biochar-based adsorbents: State-of-the-art, challenges, and future perspectives. J Environ Manag 317. https://doi.org/10.1016/j.jenvman.2022.115356. Academic Press

Slokar YM, Majcen Le Marechal A (1998) Methods of decoloration of textile wastewaters. Dyes Pigm 37(4):335–356. https://doi.org/10.1016/S0143-7208(97)00075-2

Sumalinog DAG, Capareda SC, de Luna MDG (2018) Evaluation of the effectiveness and mechanisms of acetaminophen and methylene blue dye adsorption on activated biochar derived from municipal solid wastes. J Environ Manage 210:255–262. https://doi.org/10.1016/j.jenvman.2018.01.010

Sun L, Wan S, Luo W (2013) Biochars prepared from anaerobic digestion residue, palm bark, and eucalyptus for adsorption of cationic methylene blue dye: characterization, equilibrium, and kinetic studies. Biores Technol 140:406–413. https://doi.org/10.1016/j.biortech.2013.04.116

Suteu D, Zaharia C, Badeanu M (2015) Kinetic modeling of dye sorption from aqueous solutions onto apple seed powder. Cellulose Chem Technol 50(9–10):1085–1091

Syed Z, Guerin PM (2004) Tsetse flies are attracted to the invasive plant Lantana camara. J Insect Physiol 50(1):43–50. https://doi.org/10.1016/j.jinsphys.2003.09.007

Tarekegn MM, Balakrishnan RM, Hiruy AM, Dekebo AH (2021) Removal of methylene blue dye using nano zerovalent iron, nanoclay and iron impregnated nanoclay – a comparative study. RSC Adv 11(48):30109–30131. https://doi.org/10.1039/D1RA03918K

Tran TH, Le AH, Pham TH, Nguyen DT, Chang SW, Chung WJ, Nguyen DD (2020) Adsorption isotherms and kinetic modeling of methylene blue dye onto a carbonaceous hydrochar adsorbent derived from coffee husk waste. Sci Total Environ 725:138325. https://doi.org/10.1016/j.scitotenv.2020.138325

Yang W, Wang Y, Shang J, Liu K, Sharma P, Liu J, Li B (2017a) Antagonistic effect of humic acid and naphthalene on biochar colloid transport in saturated porous media. Chemosphere 189:556–564. https://doi.org/10.1016/j.chemosphere.2017.09.060

Yang W, Wang Y, Sharma P, Li B, Liu K, Liu J, Flury M, Shang J (2017b) Effect of naphthalene on transport and retention of biochar colloids through saturated porous media. Colloids Surf, A 530:146–154. https://doi.org/10.1016/j.colsurfa.2017.07.010

Yang W, Bradford SA, Wang Y, Sharma P, Shang J, Li B (2019a) Transport of biochar colloids in saturated porous media in the presence of humic substances or proteins. Environ Pollut 246:855–863. https://doi.org/10.1016/j.envpol.2018.12.075

Yang W, Shang J, Sharma P, Li B, Liu K, Flury M (2019b) Colloidal stability and aggregation kinetics of biochar colloids: Effects of pyrolysis temperature, cation type, and humic acid concentrations. Sci Total Environ 658:1306–1315. https://doi.org/10.1016/j.scitotenv.2018.12.269

Yao Y, Xu F, Chen M, Xu Z, Zhu Z (2010) Adsorption behavior of methylene blue on carbon nanotubes. Biores Technol 101(9):3040–3046. https://doi.org/10.1016/j.biortech.2009.12.042

Publisher's Note